NEW TECHNIQUES FOR DIFFUSING-WAVE SPECTROSCOPY

T.G. Mason[a,b] Hu Gang,[b] A.H. Krall[b] and D.A. Weitz[b]

a. Dept. of Physics, Princeton University, Princeton NJ 08544.
b. Exxon Research and Engineering Co., Rt. 22E Annandale, NJ 08801.

ABSTRACT

We present two new types of measurements that can be made with diffusing-wave spectroscopy, a form of dynamic light scattering that applies in the limit of strong multiple scattering. The first application is to measure the frequency-dependent linear viscoelastic moduli of complex fluids using light scattering. This is accomplished by measuring the mean square displacement of probe particles using DWS. Their response to thermal fluctuations is determined by the fluctuation-dissipation relation, and is controlled by the response of the surrounding complex fluid. This response can be described in terms of a memory function, which is directly related to the complex elastic modulus of the system. Thus by measuring the mean square displacement, we are able to determine the frequency dependent modulus. The second application is the measurement of shape fluctuations of scattering particles. This is achieved by generalizing the theory for DWS to incorporate the effects of amplitude fluctuations in the scattering intensity of the particles. We apply this new method to study the thermally induced fluctuations in the shape of spherical emulsion droplets whose geometry is controlled by surface tension.

A microgravity environment has significant potential benefits for a wide variety of scientific problems involving colloidal particles or other complex fluids, where sedimentation can play an important role. Several experiments are currently planned to exploit this environment. Laser light scattering is an important experimental technique for studying the physics of these complex fluids; as a result a laser light scattering apparatus is being constructed by NASA to allow measurements of different types to be made in space. This apparatus will allow the traditional light scattering techniques to be employed, including both static and dynamic light scattering. In addition, the apparatus will allow several ancillary measurements to be performed. Among the most important is the measurement of the rheological properties of the complex fluids being studied. Currently this measurements will be done by mechanically agitating the sample cell and measuring the response of the complex fluid. This will provide a measure of the complex, frequency-dependent linear viscoelastic modulus of the suspension, $G^*(\omega) = G'(\omega)+iG''(\omega)$. Here, the real part, $G'(\omega)$, reflects the energy storage or the elastic component of the modulus, while the imaginary part, $G''(\omega)$, reflects the viscous dissipation of the modulus. While these mechanical measurements of the modulus provide a direct measure of the viscoelastic response of the fluid, they are limited in the frequency range that is accessible. Moreover, since the primary function of the NASA apparatus is light scattering, a preferable method for measuring the visco-elastic response would be to use light scattering techniques.

In this paper, we discuss a new method for measuring the viscoelastic response of a complex fluid using solely light scattering methods. We discuss the use of diffusing-wave spectroscopy (DWS), which is form of dynamic light scattering applicable in the strongly multiple scattering limit[1,2]. Two new applications of DWS are presented. We first discuss the use of DWS, or more traditional dynamic light scattering techniques, to measure the frequency-dependent linear viscoelastic modulus of complex fluids. We also discuss the extension of DWS to include amplitude fluctuation due to the fluctuating shape of the scattering particles, and use this to measure the shape fluctuations of emulsion droplets, where surface tension controls the spherical shape of the particles.

We begin by presenting a novel method for measuring the linear viscoelastic properties of a complex fluid over an extended range of frequencies. We show that the response of the fluid to thermal fluctuations, as probed by the average motion of small particles dispersed within the fluid, provides a very close representation of the response of the bulk fluid to an imposed shear strain. The essential physics of this approach is that the bulk mechanical susceptibility of the fluid appropriately describes the microscopic viscoelastic forces acting on a small particle excited by the thermal stochastic forces which lead to Brownian motion. By describing the stochastic motion of the small probe particle with a Langevin equation generalized to include viscoelasticity and imposing energy equipartition using the fluctuation-dissipation theorem, the average particle motion, given by the mean square displacement, $\langle \Delta r^2(t) \rangle$, determines the time-dependent memory function, $\zeta(t)$, of both the surrounding and bulk complex fluid. This time-dependent memory function is proportional to the more commonly encountered stress relaxation modulus and contains the same information as $G^*(\omega)$. We use dynamic light scattering to measure $\langle \Delta r^2(t) \rangle$, and compare the $G^*(\omega)$ obtained with that measured directly by mechanical means using a rheometer.

We describe the motion of a small, neutrally buoyant particle dispersed in a complex fluid by means of a generalized Langevin equation,

$$m\dot{v}(t) = f_B(t) - \int_0^t \zeta(t-\tau)v(\tau)d\tau \qquad (1)$$

where m is the particle mass and $v(t)$ is the particle velocity. This equation expresses the balance of forces on the particle, relating the stochastic Brownian forces, $f_B(t)$, to the response of the surrounding fluid, which is described by a generalized time-dependent memory function, $\zeta(t)$, and reflects the dependence of the properties of the material at time t on the behavior at previous times. A simplified form of this equation is commonly used to describe the motion of a particle in a purely dissipative viscous fluid; here we generalize it by using the memory function to describe the average, effective-medium response of a complex fluid that can also store energy. Allowing the medium to store energy profoundly changes the temporal correlation of stochastic forces acting on the particle at thermal equilibrium. Because energy from thermal fluctuations can be stored in the medium over time scales determined by the memory function, the dissipation required to maintain thermal equilibrium also occurs over these time scales. As a result, the stochastic forces acting on the particle are correlated over finite rather than infinitesimal time scales to prevent an unphysical energy buildup. Thus, the fluctuation-dissipation theorem differs from the commonly encountered delta-function correlation of a purely viscous fluid, and here takes the form[3]:

$$\langle f_B(0)f_B(t)\rangle = k_B T\zeta(t) \qquad (2)$$

where the coefficient ensures thermal equilibrium, with k_B Boltzmann's constant and T the temperature.

By taking the Laplace transform of Eq. (1), and using Eq. (2), the viscoelastic memory function can be related to the velocity autocorrelation function, and, hence, the mean square displacement of the particle. We assume that the Laplace transform of the microscopic memory function is proportional to the bulk frequency-dependent viscosity, $\tilde{\eta}(s) = \tilde{\zeta}(s)/6\pi a$, where s represents the frequency in the Laplace domain. We choose the coefficient to ensure the correct Stokes drag on a particle of radius, a, in a purely viscous fluid, recognizing that this coefficient may differ somewhat in describing the behavior of a particle in a viscoelastic fluid. The frequency-dependent shear modulus is directly related to the viscosity by $\tilde{G}(s) = s\tilde{\eta}(s)$, and hence to the mean square displacement, $\langle \Delta\tilde{r}^2(s)\rangle$:

$$\tilde{G}(s) = \frac{s}{6\pi a}\left[\frac{6k_BT}{s^2\langle \Delta\tilde{r}^2(s)\rangle} - ms\right] \qquad (3)$$

The terms within the brackets come from the solution of the Langevin equation for the memory function, $\tilde{\zeta}(s)$; the first captures the thermal fluctuation-dissipation in the medium surrounding the particle, while the second is due to the particle's inertia. In most complex fluids, the inertial term is negligible compared to the fluctuation-dissipation term, except at very high frequencies. Fitting the optically measured $\tilde{G}(s)$ with an appropriate functional form, the complex, frequency-dependent shear modulus can be determined using analytic continuation by setting $s = i\omega$, and identifying $G'(\omega)$ and $G''(\omega)$ as the real and imaginary parts. Provided the functional form describes $\tilde{G}(s)$ over all measured frequencies, the Kramers-Kronig relationship will be satisfied over the measured range of frequencies. The complete procedure establishes a very general relationship between the mean square displacement of suspended particles and the bulk rheological properties of the complex fluid surrounding them.

To test the applicability of this scheme, we use diffusing-wave spectroscopy to determine the mean square displacement of the particles in a concentrated suspension of silica particles of relatively uniform radius, $a = 0.21$ μm, suspended in ethylene glycol. These particles behave essentially as hard spheres. Their volume fraction was increased by centrifugation to $\phi \approx 0.56$, quenching in disorder, to form an isotropic hard sphere glass. Diffusing-wave spectroscopy was used in the transmission geometry to measure the correlation function for a 4-mm thick sample, shown in Fig. 1; characteristic of a colloidal hard sphere glass, it exhibits an initial, rapid decay to a plateau value, followed by a final decay at longer times. The particles are relatively small, so that DWS is slightly sensitive to collective motion; nevertheless to a good approximation the correlation function can be inverted to obtain the mean square displacement of the particles. This requires knowledge of the transport mean free path of the light, l^*, which was obtained from static transmission measurements. The mean square displacement obtained from the correlation function is shown in Fig. 2. The linear increase at the shortest times reflects the initial diffusive motion of the particles; at longer times their motion is constrained by the local cage structure of the colloidal glass. The decay in the correlation function at the longest times can not be simply interpreted as a mean square displacement of individual particles setting the upper bound on the data accessible.

We numerically calculate the Laplace transform of the mean square displacement, and use Eq. (3) to determine $\tilde{G}(s)$, which is shown by the open points in Fig. 3. The accuracy of the Laplace transform is limited at the shortest and the longest time scales because of the limits of the available data. Nevertheless, the data exhibit

several very general features that characterize $\tilde{G}(s)$. The region having relatively low slope at lower frequencies indicates energy storage and hence a range where the real component of the complex modulus dominates. The region having nearly unity slope at higher frequencies indicates viscous dissipation, and hence a range where the imaginary component of the complex modulus dominates. This is very generally true of the data for $\tilde{G}(s)$; regions of small slope indicate that the elastic component of the modulus dominates, while regions of near-unity slope indicate that the viscous component dominates; the deviations from these slopes reflect contributions from both components.

To obtain the real and imaginary parts of the complex modulus, the frequency-dependent magnitude given by $\tilde{G}(i\omega)\tilde{G}(-i\omega) = \left|G^*(\omega)\right|^2$ can be fit using a superposition of complex moduli which satisfy the Kramers-Kronig relationship and have a single Maxwellian relaxation time. Rather than follow this more general procedure, we instead use our physical intuition about the behavior expected for a colloidal hard sphere glass to determine $\tilde{G}(s)$. We include a constant to account for the elasticity at low frequencies; a term proportional to $s^{0.3}$ to account for the behavior of the plateau, as predicted by mode coupling theories[4]; a term proportional to $s^{0.5}$ to account for the predicted asymptotic high frequency elastic modulus of hard spheres [5]; and a term proportional to s to account for the high frequency viscous component. A fit to a sum of these terms yields the solid line in Fig. 3. The real and imaginary components of $G^*(\omega)$ can then be calculated directly. Due to the form of $\tilde{G}(s)$, these do not satisfy Kramers-Kronig at low frequencies, but they do properly predict the moduli within the limits of the measured data.

To compare the elastic moduli calculated from the light scattering data with those determined directly by an oscillatory mechanical measurement, we use a controlled strain rheometer with a double-wall Couette sample cell geometry. A small, sinusoidal strain was applied and the in and out of phase components of the resultant stress were determined as the frequency was varied. The amplitude of the strain was maintained well below 1% to ensure that the data were obtained in the linear regime; this was verified by varying the strain amplitude. The upper frequency was limited by the motor's ability to produce a reliable sinusoidal strain, while the lower frequency was limited by the sensitivity of the torque transducer. The resultant real and imaginary components of the complex modulus are shown in Fig. 4. The dashed lines show the values of $G'(\omega)$ and $G''(\omega)$ obtained from the light scattering data. Remarkably good agreement is found, except for the loss modulus at the lowest frequencies. The light scattering data represent the overall trend of the rheological data quite well, particularly for the larger storage modulus.

These results clearly illustrate the possibility of using light scattering methods to determine the visco-elastic response of a suspension of hard spheres. We have also successfully tested the technique on very different forms of complex fluids, including polymer solutions and concentrated emulsions; in all cases tried the results are in good agreement with the mechanical measurements. The essential physics of this technique relies on the equivalence of the frequency-dependence of the microscopic memory function which describes the response of a probe particle in the complex fluid and the macroscopic complex viscoelasticity of the complex fluid. Provided particle inertia can be ignored and the viscoelastic coupling between neighboring particles varies as q^2, the complete equations of motion for a lattice of interacting particles can be reduced on average to a single particle equation of motion like the generalized Langevin equation having a memory function which describes the average bulk dynamics inherent in the microscopic coupling. This equivalence is perhaps somewhat surprising; the motion of a probe particle, as probed by light scattering normally reflects relatively large wavevector, q, behavior. Moreover, light scattering typically probes the longitudinal response of a system. By contrast, the elastic modulus of a material reflects the transverse response of the material in the limit of $q \to 0$. However, the mean square displacement does couple to shear modes; this is certainly true in the limit of a simple viscous fluid, where the shear viscosity determines the particle's motion. Thus, by analogy, we expect the shear elasticity of a complex fluid to determine the mean square displacement of a probe particle. However, the elasticity is typically measured by applying a uniform strain across the material; this is not the case for a small probe particle. As a result, the flow pattern of the viscoelastic fluid around the particle may differ significantly from the case of a simple viscous fluid; this will modify the coefficient relating the viscosity to the memory function, and may even make it frequency dependent. Thus, this method may not provide quantitatively exact measures of the elastic moduli; nevertheless, the overall trends are captured, and, as shown by our results, the agreement is surprisingly good.

Perhaps most importantly, this method provides a measure of the elastic moduli over a much broader range of frequencies than is obtained with mechanical measurements. Moreover, it provides a convenient method to relate the energy storage and loss due to strain to the microscopic mean square displacement of the particles in the suspension. These two advantages can provide considerable new insight into the underlying physics of the complex fluid. For example, for the hard sphere suspension, the plateau in $\left\langle \Delta r^2(t) \right\rangle$ is known to reflect the quenched disorder of a colloidal glass; the particle can diffuse freely at very short length scales until it reaches the cage formed by the

neighboring particles. Then the particle motion is restricted until the cage decays at much longer time scales. This behavior is accounted for theoretically by mode coupling theory (MCT) [4,6]. Our results indicate that the cage effects also play an important role in the rheological behavior of a hard sphere suspension; the existence of the cage leads to an additional mechanism for energy storage; presumably the strain distorts the shape of the cage, allowing energy to be stored, and causing the real part of the complex modulus to dominate. Mode coupling theory accounts for this behavior at high frequencies and predicts a β-relaxation contribution proportional to $s^{0.3}$ in addition to a constant nonergodicity parameter which characterizes the low frequency plateau elasticity. This $s^{0.3}$ component improves our fit to the transformed light scattering data, and directly contributes to the frequency dependence of the storage modulus. In fact, the predictions of MCT can be used to better describe the behavior of the loss modulus at lower frequencies. The rise in $G''(\omega)$ measured mechanically suggests an additional decay process at lower frequencies; MCT predicts that this α-relaxation process, or von Schweidler decay, results from the ultimate cage breakup at long times, and provides a functional form to describe it, suggesting an additional term proportional to $s^{-0.55}$ in $\tilde{G}(s)$. Subtracting this α-decay term leads to much better agreement at low frequencies between $G''(\omega)$ obtained from light scattering and that measured rheologically, as shown by the solid line in Fig. 4.

The second new application of DWS discussed here is the generalization of the theory for the technique to include amplitude fluctuations of the scattering particles. We use this scattering method to study the thermally driven shape fluctuations of monodisperse emulsion droplets, and to determine the effects of increasing volume fraction on the fluctuations. The thermally induced increase in the surface area of a fluid droplet is $\Delta R^2 \approx k_B T/\Gamma$, where Γ is the surface tension. For a typical surface tension of 10 dynes/cm, this corresponds to an increased area of only about 30 $Å^2$; for a 1 μm diameter droplet, this represents a change in the radius of less than 0.1%. The relaxation time, τ, of these fluctuation is also very rapid; it is determined by the viscosity of the two fluids. If the viscosity of the droplet is much greater than that of the continuous phase, the relaxation time is $\tau \approx R\eta/\Gamma$; for $\eta = 0.1$ P and $R \approx 1$ μm, $\tau \approx 10^{-6}$ sec. The combination of the very short time scale and the very small amplitude of the thermal fluctuations of emulsion droplets have, to date, precluded their observation.

Our samples are emulsions of silicone oil in water, stabilized with sodium dodecylsulphate, and purified using the technique of fractionated crystallization to yield highly monodisperse droplets with a radius of $R = 1.4$ μm[7]. The surface tension of the interfaces is measured to be 9.8 dynes/cm. We perform our DWS measurements in the transmission geometry using an expanded beam from an Ar^+ laser, which gives $k_0 = 16.3$ μm^{-1} for the incident wavevector in water. The detected light is collected from a point on the exit side of the 5-mm-thick sample cell. The transport mean free path, l^*, is determined independently by a static transmission measurement [2], allowing the correlation function to be inverted to determine the dynamics of the individual emulsion droplets [8].

We might expect the dynamics of emulsion droplets to be the same as those of hard spheres. This is indeed the case for an emulsion made of a high viscosity oil, $\eta = 1000$ cP. This is illustrated in Fig. 5, where the open circles represent $\langle \Delta r^2(t) \rangle$, the mean square displacement of an individual droplet. The data follow the shape predicted for hard spheres, shown by the solid line. By contrast, an emulsion made from a much lower viscosity oil, $\eta = 12$ cP, exhibits distinct additional dynamics, as shown for $\phi = 0.35$ by the solid circles in Fig. 5. At early times, the data are significantly higher than those expected for solid spheres; at later times the data merge. Similar behavior is observed for all ϕ. These additional dynamics result from the shape fluctuations; for the higher η, the relaxation time is so long that any shape fluctuations are masked by the large displacements that occur during τ.

To quantitatively describe these new dynamics, we must generalize the formalism for DWS to include fluctuations in the scattering *amplitude*, in addition to the phase fluctuations which result from translational motion. The analysis of the correlation function measured by DWS entails the calculation of the contribution of diffusive light paths comprised of a large number of scattering events; these are all represented by an angle-averaged scattering event [2]. Thus, to include the amplitude fluctuations, we write the correlation function for this q-averaged, scattering event as

$$g_1(t) = \frac{\langle b^*(q,t)b(q,0)\rangle_q}{\langle b^*(q,0)b(q,0)\rangle_q} \langle \exp\{-i\vec{q}\cdot\Delta\vec{r}(t)\}\rangle_q \quad . \tag{4}$$

Here, the time dependent scattering amplitude is $b(q,t)$, and the brackets with the subscript q denote an ensemble and q-average. We assume that the amplitude fluctuations are independent of the translational motion of the droplets, and we neglect the effects of correlations between the particles [9]. The amplitude fluctuations contribute an additional correlation function which is assumed to consist of a sum of a constant portion and a much smaller fluctuating portion. Performing the q-average,

$$g_1(t) = \left[\frac{\sigma_0 + \Delta\sigma(t)}{\sigma_0 + \Delta\sigma(0)}\right] \exp\left\{-\frac{k_0^2 l}{3l^*}\left\langle \Delta r^2(t)\right\rangle\right\}, \tag{5}$$

where σ_0 is the total cross section and $\Delta\sigma(t)$ is the correlation function of the fluctuating portion of $b(q,t)$, ensemble and q-averaged. We have also used the relationship, $\left\langle q^2\right\rangle_q = k_0^2 l / 2l^*$, where l is the scattering mean free path [10].

To calculate the correlation function for a diffusive path of length s, consisting of $n = s/l$ scattering events, we take the product of Eq. (5) n times [2]. Since $\Delta\sigma(t) \ll \sigma_0$, the first term can be approximated as an exponential, $\exp\{(\Delta\sigma(t)-\Delta\sigma(0))/\sigma_0\}$; this ensures that the contribution of a single diffusive path is still linear in s, and allows the standard DWS analysis to be retained. Thus, the total DWS correlation function is a sum over the contributions of all paths, weighted by the probability that a photon follows the path, $P(s)$:

$$g_1(t) = \int P(s) \exp\left\{-\frac{sk_o^2}{3l^*}\left[\left\langle \Delta r^2(t)\right\rangle + \frac{3l^*}{lk_o^2}\frac{\Delta\sigma(0)-\Delta\sigma(t)}{\sigma_o}\right]\right\} ds. \tag{6}$$

Since $P(s)$ is known [2], this equation can be solved in exactly the same manner as done for DWS from solid particles. The effects of the amplitude fluctuations are contained in the second term in the square brackets. It is clear from Eq. (6) that DWS probes the relative fluctuations of the cross section; like $\left\langle \Delta r^2(t)\right\rangle$ their contribution increases from zero at t=0 but saturates at long times. It is also clear why very small fluctuations can be detected; the signal arises from the sum of n independent amplitude fluctuations. These minute fluctuations would not be detectable without the advantage of the multiple scattering.

We note that this derivation is independent of the nature of the amplitude fluctuations; not only shape fluctuations, but other phenomena, such as rotational motion of aspherical particles can also result in a similar contribution. Moreover, the DWS data can be inverted, and the translational and amplitude contributions can be separated. We do this here by subtracting the translational motion; the full effects of the hydrodynamic interactions are included by using the scaling form which describes the data for solid spheres [8]. We plot $R^2\Delta\sigma(t)/\sigma_0$ for ϕ = 0.35 in Fig. 6; we multiply the normalized fluctuating cross section by R^2 to give the correlation function of the fluctuations of the droplet radius. We note that the data exhibit a distinctly non-exponential decay.

Similar behavior is found for all other droplet volume fractions. Surprisingly, the shape of the correlation function is independent of ϕ; all the data can be scaled onto a single master curve. This enables us to determine the ϕ-dependence of the shape fluctuations. We find that the characteristic frequency of the decay decreases approximately linearly with increasing volume fraction, as shown by the open triangles in Fig. 6. By contrast, we find that the amplitude of the shape fluctuations increase dramatically with ϕ; this is shown by the solid circles in Fig. 6.

To quantitatively describe the correlation function of the fluctuating shape, we expand the instantaneous radius of the drop in spherical harmonics [11]. Each independent deformation mode creates an excess area given by $k_BT/2\Gamma$. Together with the conservation of volume, this condition determines the amplitude of the expansion coefficients. Each mode relaxes independently with an exponential decay rate, ω_l, that must be calculated in the overdamped, or low Reynolds number, limit [12]. We obtain

$$\Delta\sigma(t) = \frac{k_BT}{4\pi\Gamma R^2}\sum_{l=2}\frac{2l+1}{l(l+1)-2} g_l \exp(-\omega_l t), \tag{7}$$

with

$$\omega_l = \frac{l(l+2)(2l+1)}{2\left(2l^2+4l+3\right)}\frac{\Gamma}{\eta R}. \tag{8}$$

In general, ω_l depends on the viscosities of both fluids [13]; here we have assumed that the viscosity of the oil is much greater than that of the water. Note that asymptotically $\omega_l \sim l$, reflecting the fact that the dynamics are driven by surface tension; by contrast, $\omega_l \sim l^3$ when the dynamics are driven by the interfacial rigidity [11]. The cross section for each mode is calculated within the Rayleigh-Gans (RG) approximation [14],

$$g_l = \pi\int_0^{\pi} \sin\theta\left(1+\cos^2\theta\right)\left[3j_l(x)\right]^2 d\theta, \tag{9}$$

where $x = 2k_0R\sin(\theta/2)$, and where we have omitted an optical constant which is canceled in the normalization by σ_0. The coefficients, g_l, depend only on k_0R, and become negligible when $l \gg k_0R$, since the length scale of the features described by such modes is much smaller than the wavelength of the radiation. This sets the upper bound to the expansion; we find that the series converges for $l \approx 20$. Because of their large mismatch in index of refraction, Mie theory, suitably generalized to treat non-spherical scatterers, should be used. However, the average cross section

calculated within the RG approximation differs by less than 0.5% from that calculated using Mie theory. Thus, we conclude that the RG approximation is sufficiently accurate.

These expressions apply only to an isolated droplet. However, since the functional form of our data is independent of ϕ, we can use them to describe all the data by allowing both the characteristic frequency and the amplitude to vary. The solid line through the data in Fig. 6 illustrates the fit for ϕ=0.35. Excellent agreement is obtained. The non-exponential decay clearly reflects the contribution of the different modes. Quantitative agreement between the theory and the experiment should be obtained when the ϕ-dependent characteristic frequency, $\omega(\phi)$, and amplitude, $\Delta\sigma(\phi)$, are extrapolated to zero volume fraction. Our extrapolated value of $\omega(\phi)$ is identical to the predicted value of $\Gamma/\eta R$ = 1.2 MHz. Similarly, the extrapolated value of the amplitude ratio $R^2\Delta\sigma(0)/\sigma_0$ is 65 Å^2, in good agreement with the predicted value of $(k_BT/4\pi\Gamma\sigma_0)\Sigma(2l+1)g_l/(l(l+1)-2)$ = 52 Å^2. The remaining discrepancy may reflect the error introduced by the RG approximation.

The ϕ-dependence of both the frequency and the amplitude must reflect the consequences of the interactions between the droplets, and these are not, as yet, well understood theoretically. The normalized characteristic frequency is well represented by a linear behavior, $\omega(\phi)/\omega(0)$=1-0.78ϕ. The frequency depends only on the surface tension, R, and the viscosities of the two liquids; it is unlikely that Γ changes with ϕ, so that the most likely origin of this behavior is the ϕ-dependence of the effective viscosity of the emulsion. A similar linear form was recently predicted for the l=2 modes, but the predicted coefficient is 1.4 [15]. However, this theory was restricted to the case of equal viscosities of the oil and water, which may account for the discrepancy.

The pronounced ϕ-dependence of the amplitude of the shape fluctuations is more surprising. This may reflect the effects of collisions between the droplets, which become increasingly likely as ϕ increases; because the droplets are flexible, these collisions may result in additional deformations. We model the effects of collisions by introducing a contribution to the amplitude proportional to the fraction of the droplets that, at any instant, are colliding with a neighbor. This fraction we estimate as $\phi g(2,\phi)$, where $g(2,\phi)$ is the pair correlation function at contact. The dashed line through the data in Fig. 6 is a fit of $\Delta\sigma(\phi)/\Delta\sigma(0)$ to the functional form $1+C\phi g(2,\phi)$ with $g(2,\phi)=(1-\phi/2)/(1-\phi)^3$ as holds for hard spheres [16]. Good agreement is found with C=1.7, suggesting that colliding droplets deform an extra amount that is about 1.7 times the deformation exhibited by an isolated droplet. More generally, it should be possible to regard these increased shape fluctuations as the consequence of the osmotic pressure of flexible spheres. The expression $1+C\phi g(2,\phi)$, with C=4 and $g(2,\phi)$ as given above, is in fact the ratio of the full osmotic pressure of a hard-sphere suspension to the kinetic part nk_BT, where n is the number density [16]. This observation suggests that $\Delta\sigma(\phi)/\Delta\sigma(0)$ may be related to the reduced osmotic pressure of the flexible droplets.

The results presented here are two extensions of DWS. Amplitude fluctuations can arise from many phenomena in addition to the shape fluctuations presented here; for example, rotational diffusion of aspherical particles will also lead to similar effects, and the theory presented here should be applicable. The ability to measure the linear viscoelastic modulus optically enables its determination over a much broader frequency range, without mechanical motion. This could be particularly beneficial for experiments studying complex fluids in microgravity.

We gratefully acknowledge very useful discussions with T. Lubensky, R. Klein, W. Russel, W. Graessley, J. Bibette, S. Milner and W. Cai.

REFERENCES:

1. Maret, G. and Wolf, P., *Z. Phys.* **B65**, 409 (1987).
2. Pine, D.J., Weitz, D.A., Chaikin, P.M. and Herbolzheimer, E., *Phys. Rev. Lett.* **60**, 1134 (1988).
3. Chaikin, P.M. and Lubensky, T., *Principles of Condensed Matter Physics*, (Cambridge University, Cambridge, 1994).
4. Gotz, W. and Sjogren, L., *Phys. Rev.* **A43**, 5442 (1991).
5. van der Werff, J., de Kruif, C., Blom, C. and Mellma, J., *Phys. Rev.* **A39**, 795 (1989).
6. van Megen, W. and Pusey, P.N., *Phys. Rev.* **A43**, 5429 (1991).
7. Bibette, J., *J. Coll. Interface Sci.* **147**, 474 (1991).
8. Zhu, J.X., Durian, D.J., Muller, J., Weitz, D.A. and Pine, D.J., *Phys. Rev. Lett.* **68**, 2559 (1992).
9. Weitz, D.A., Zhu, J.X., Durian, D.J., Gang, H. and Pine, D.J., *Physica Scripta* **T49**, 610 (1993).
10. Wolf, P.E., Maret, G., Akkermans, E. and Maynard, R., *J. Phys. (Paris)* **49**, 63 (1988).
11. Milner, S.T. and Safran, S.A., *Phys. Rev.* **A36**, 4371 (1987).
12. Cox, R.G., *J. Fluid Mech.* **37**, 601 (1969).
13. Choi, S.J. and Schowalter, W.R., *Physics of Fluids* **18**, 420 (1974).
14. Huang, J.S., Milner, S.T., Farago, B. and Richter, D., *Phys. Rev. Lett.* **59**, 2600 (1987).
15. Schwartz, M. and Edwards, S.F., *Physica A* **167**, 589 (1990).
16. Brady, J.F., *J. Phys. Chem.* **99**, 567 (1993).

FIGURES

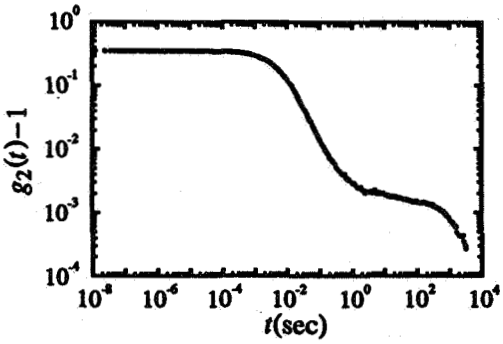

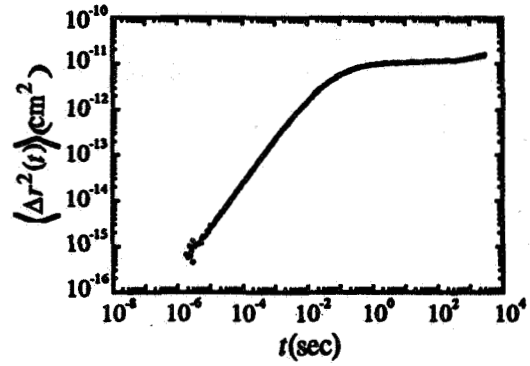

Fig. 1 (LEFT) DWS autocorrelation function for a suspension of hard sphere colloids at $\phi \approx 0.56$.

Fig. 2 (RIGHT) Mean square displacement of hard spheres determined from the data in Fig. 1. At early times the particles diffuse; at later times the particles are trapped in cages formed by the neighboring particles.

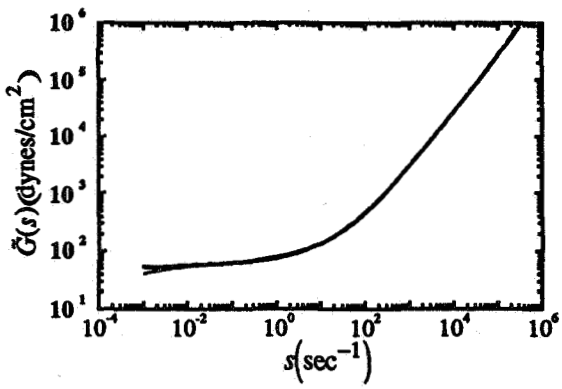

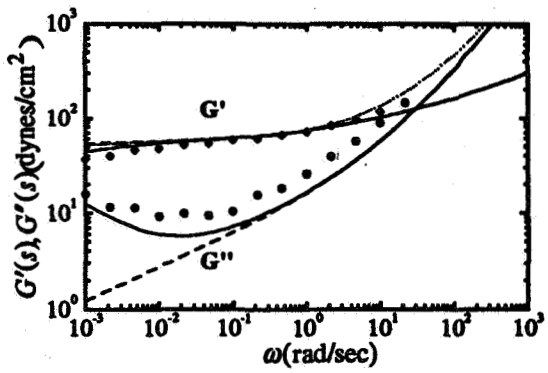

Fig. 3 (LEFT) Laplace transform of the complex modulus, $\tilde{G}(s)$, determined from the mean square displacement, shown in Fig. 2, for hard sphere colloids.

Fig. 4 (RIGHT) Comparison of the complex moduli for hard sphere colloids determined with light scattering (solid lines) and with a rheometer (points). The dashed line does not include a decay at longer time; the solid line does. The light scattering data are determined from the $\tilde{G}(s)$ shown in Fig. 3.

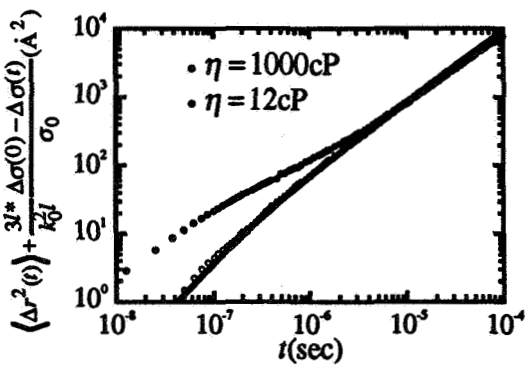

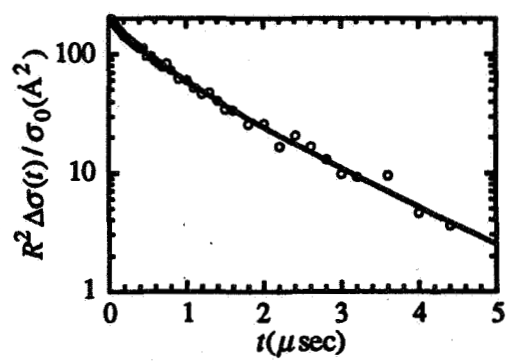

Fig. 6. (LEFT) Inverted correlation functions of monodisperse emulsions. The data are the sum of the mean square displacement and a term related to the correlation function of the fluctuating scattering amplitude. The solid points are for an emulsion with an oil viscosity of 12 cP, while the open points are for an emulsion with an oil viscosity of 1000 cP. The solid line is the theoretical prediction for rigid spheres.

Fig. 6. Correlation function of the radius fluctuations of an emulsion with $\phi = 0.35$, compared with theory.

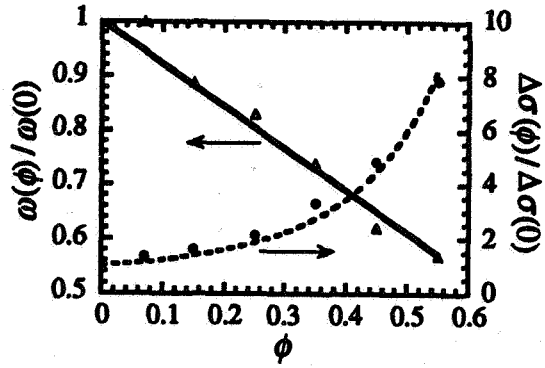

Fig. 7. The ϕ-dependence of the characteristic frequency (open triangles) and the fluctuating amplitude (solid circles). Both quantities have been reduced by their extrapolations to zero volume fraction. The solid line is a fit to a linear decay, with a coefficient of 0.78; the dashed line is a fit to a simple model which attempts to include the effects of interactions between the droplets.